

# Optimizing Grid-Integrated Renewable Systems for Cost-Effective Electricity and Hydrogen Supply

Sarad Basnet<sup>◇</sup>, Karine Deschinkel<sup>◇</sup>, Luis Le Moynes\*, Marie Cécile Péra<sup>◇</sup>  
<sup>◇</sup>Université de Franche-Comté, CNRS, institut FEMTO-ST, F-90000 Belfort, France  
\*Université de Bourgogne, ISAT, Drive, 58000 Nevers, France

**Abstract**—This study analyzes the technical and economic feasibility of a hybrid renewable energy system consisting of solar photovoltaic (PV), wind (WT), grid, battery (Bt), electrolyzer, hydrogen tank (H<sub>2</sub> tank), and fuel cell to meet the electricity and hydrogen needs based on the real data of Dijon, France. Mixed-integer linear programming (MILP) integrated inside an open-source Python FINE module is employed to optimize the design and operation of an energy system. Three different case studies are performed; Case I: Grid, Bt, H<sub>2</sub> components, Case II: Grid, WT, PV, Bt, H<sub>2</sub> components, Case III: WT, PV, Bt, H<sub>2</sub> components (off-grid). The major objective of the study is to minimize the total annual cost (TAC) of the system in every case study. The optimization results indicate the difference in TAC based on the operation and choice of various components. In Case I, the TAC is observed to be 52.82 million euros, focusing solely on the grid operation without considering any grid investment. For Case II, the TAC is found risen to 163 million euros due to significant investments in PV and WT. In Case III, a substantial TAC of 1790.85 million euros is obtained, attributed to major investments in PV, WT, Bt, H<sub>2</sub> tank, and fuel cell. The study shows that utilizing the grid in combination with renewable sources such as wind and photovoltaic currently can be the cost-effective solution, while solar and wind energy may become more competitive if investment and operating costs decrease. Furthermore, batteries and hydrogen tanks are identified as suitable storage technologies for supporting the peak electricity and hydrogen demand of energy systems. Fuel cell is still an expensive choice however, the future development in fuel cell technologies holds the potential for more affordable power solutions.

**Keywords**—H<sub>2</sub> Hybrid renewable energy system, MILP optimization, Python FINE module

## I. INTRODUCTION

The increasing demand for clean and sustainable energy has led to the development of hybrid renewable energy systems (HRES) that integrate various renewable energy sources, such as photovoltaic (PV), wind turbines (WT), biomass (BM), hydropower (HP), geothermal energy (GE), etc. PV and WT are commonly used because of their global availability and mature technology. However, their intermittent nature consistently poses challenges in meeting energy demands [1]. To address this issue, PV and WT are often integrated with generators (Gn) or storage technologies such as batteries (Bt), and hydrogen tank storage (H<sub>2</sub> tank) to avoid short/long-term energy fluctuation.

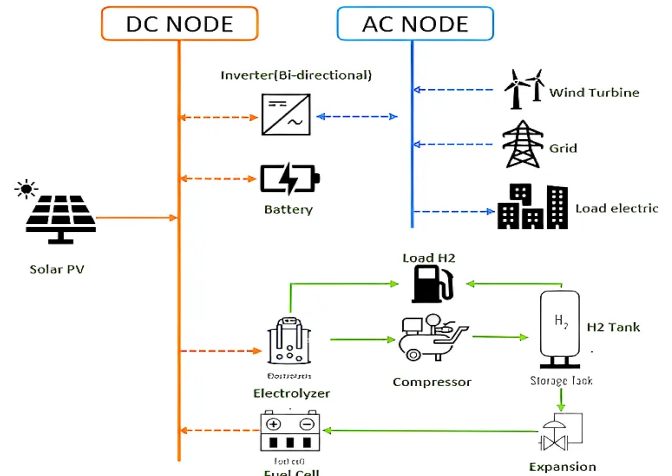


Fig. 1: System Architecture

In numerous research, diverse studies have been performed into the sizing and design optimization of Hybrid Renewable Energy Systems (HRES), encompassing PV, WT, Bt, H<sub>2</sub> system technologies both in standalone and grid-integrated configurations [2]. Study in [3] introduced a robust energy planning approach utilizing multi-objective Optimization with Non-dominated Sorting Genetic Algorithm II (NSGA-II) for a high-rise building powered by PV, WT, Bt, and H<sub>2</sub> vehicle storage. Optimal system sizing for supplying electricity to 50 residential households on Canadian islands was proposed by [4], considering cost and reliability objectives using the HOMER Pro commercial tool. Authors in [5] proposed a 100 percent renewable island energy system based on power-to-gas and biogas technologies, incorporating multi-objective scenarios of total annual costs and wasted renewable energy using k-means clustering. Authors in [6] explored grid-integrated PV, Bt, H<sub>2</sub> system with multi-objective considerations of cost, CO<sub>2</sub> emissions, and grid dependency for 1500 inhabitants near Marseille, France using sequential quadratic programming fulfilling both electric and H<sub>2</sub> demand. Study in [7] developed a two-stage multi-objective metaheuristic-TOPSIS method for designing a solar-biomass-based H<sub>2</sub> and electricity co-supply

hub, considering economic, supply stability, and waste energy generation aspects. Study in [8] presented a PV-Bt system for home appliances, minimizing annual costs using the Python pyomo optimization package. Authors in [9] investigated the sizing of PV, WT, Grid, Gn, Bt, and H<sub>2</sub> systems for a typical residential building in South Iran using the Harmony Search method and compared it with other algorithms: simulated annealing and also with commercial tool HOMER. Authors in [10] studied a PV-H<sub>2</sub> HRES for an education building and tram in Algeria, addressing a multi-objective problem through epsilon-constraints to reduce energy costs and non-renewable usage. Despite the abundance of studies, the simultaneous fulfillment of multi-energy demands for electrification of the houses/villages/buildings/cities and H<sub>2</sub> transportation has been found less. H<sub>2</sub> technologies encompassing electrolyzers, H<sub>2</sub> tanks, and fuel cells are abundantly studied in the standalone or off-grid electricity provision in which H<sub>2</sub> is used as an energy vector to mitigate seasonality arising from high demand and low renewable energy production [11], [12], [13]. In another case, it is used as fuel to power fuel cell electric vehicles [14]. In some HRES studies, both H<sub>2</sub> production for transportation and production of electricity for isolated or grid-connected households are proposed with the analysis done mostly on commercial tools like HOMER or using meta-heuristic approaches [15], [10].

In this study, simultaneous fulfillment of electricity demand and H<sub>2</sub> transportation demand is presented. For that, a distinct perspective HRES is analyzed; which includes feasible components such as PV, WT, grid, Bt, and H<sub>2</sub> system components like electrolyzer, H<sub>2</sub> tank, fuel cell, compressors, and expanders as shown in Fig 1. Unique approach of using mixed-integer linear programming (MILP) integrated into Python's "FINE" module [16] is presented based on the Pyomo optimization platform using "Gurobi™" as a solver. It is noteworthy that the FINE module, still in the development phase, distinguishes itself from conventional tools like HOMER, offering more transparency and flexibility in its application. The techno-economic analysis of an energy system is conducted for three different cases considering Dijon, France which are :

Case I: Grid, Bt, H<sub>2</sub> components

Case II: Grid, WT, PV, Bt, H<sub>2</sub> components

Case III: WT, PV, Bt, H<sub>2</sub> components (off-grid)

Dijon was chosen due to the availability of real-time electricity demand data and existing hydrogen contracts for various types of H<sub>2</sub> fueled vehicles in 2020. It also features well-developed grid infrastructure, making it conducive for a comprehensive assessment of the energy model in an urban setting.

Section II of our study introduces a comprehensive technical and economic model encompassing the various components involved. In section III, we outline the simulation and optimization process conducted for these components. We discuss the specific objectives aimed to achieve, the programming

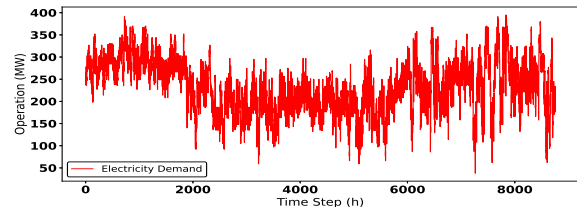


Fig. 2: Electricity demand of Dijon (MW)

interface utilized, and the solvers employed to carry out the optimization tasks effectively. Lastly, in Section IV, we present the outcomes of the study and engage in discussions surrounding the results.

## II. METHODOLOGY

The study analyzes the mentioned perspective HRES study in three different Cases I, II, and III (off-grid) based on the real data of Dijon, France. The geographic coordinates of Dijon, including latitude (47.317), longitude (5.017), time zone (UTC+1), population (159,106), area (40.41 km<sup>2</sup>), and several taxing households (155,834), provide a comprehensive picture of the urban European city. The grid infrastructure in the area is incorporated into the system architecture as it's developed and economically viable for H<sub>2</sub> production and powering houses. PV and wind systems are included due to their renewable nature, availability, and cost-effectiveness, with noted reductions in cost since 2010 according to the Renewable Energy Agency IRENA report [17]. The study considers the production of green H<sub>2</sub> via electrolysis primarily prioritizing renewable sources such as wind turbines and photovoltaics, which are feasible in case of Dijon. Produced H<sub>2</sub> is stored in the H<sub>2</sub> tank to fulfill H<sub>2</sub> demand or can be used in the fuel cell when electricity demand is high. H<sub>2</sub> is considered a potential energy carrier for the future, and the technology of H<sub>2</sub> components such as electrolyzers, H<sub>2</sub> tanks and fuel cells has been improving with a 40-60 percent decrease in costs since 2006 [18]. In this system, batteries are utilized to enhance the storage capacity and balance the short-term fluctuations in energy supply and demand. The batteries store excess energy produced by PV and wind systems during high production and discharge it later when the electricity demand is high, leading to a reduced reliance on the H<sub>2</sub> system and grid. The simulation and optimization of the studied HRES are based on technical and economic parameters. The modeling and methodology of the technical and economy of the components are elaborated in the subsequent section.

### A. Electricity and hydrogen load

The average real-time electricity demand for the city of Dijon from January 1, 2022, to December 31, 2022, was retrieved from Open Data Réseaux Énergies (ODRÉ) with a peak electrical load of 395 MW [19] as shown in Fig 2. The hydrogen (H<sub>2</sub>) demand scenario in this study is based on

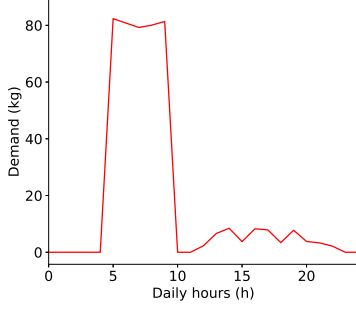


Fig. 3: Hydrogen demand of Dijon (kg/h)

a 2020 Dijon Metropole project, which involved 27 buses, 9 dumpsters, and 15 light vehicles running on hydrogen [20]. To determine the daily periodic  $H_2$  consumption of the vehicles, the total travel distance of each type of vehicle was taken into consideration. The daily pattern of  $H_2$  load is shown in Fig 3, and it was thought to remain the same every day throughout the year. The study estimated that a total of 457.35 kg of  $H_2$  per day was required to meet the  $H_2$  demand of all 51 vehicles, with a peak demand of 84.6 kg/h to refuel the bus, cars, and dumpsters in between 5 to 10 a.m. in the morning. The study took into account the fact that 49.3 kWh of electricity was required to produce one kilogram of  $H_2$  [21] and considered about 1% of random refueling activity from noon to midnight, with one percent of random refueling considered at each hour. No refueling activity was considered from midnight to 5 a.m. or from 10 a.m. to 12 p.m. The same pattern was followed throughout the year, with a standard deviation of 10.

#### B. Grid

To address the peak electricity demand, the power grid was included as a potential source of electricity. As the French mix is highly decarbonized due to the share of nuclear power, the assumption is made that the contribution of the grid is carbon-free and its capacity is unlimited.

#### C. Wind Turbine

The wind turbine model includes rated power, hub height, rotor diameter, and performance curve. In this study, we selected the GE 3.2-130 wind turbine [22], with a hub height of 110 m, a rotor diameter of 130 m, a roughness length of 0.1, and a rated power of 3.2 MW. Wind speed values for Dijon were obtained using geographic data from MERRA-2 data sources, based on geographic weather data from the National Aeronautics and Space Administration (NASA) of the United States [23]. The Windpowerlib [24] open library in Python was used to obtain wind power generation, utilizing wind turbine technology data, wind speed data, and power curves. Windpowerlib utilizes the following equation to generate the wind turbine power.

$$P_w = \frac{1}{8} \times \rho_{hub} \times d_{rotor}^2 \times v_{wind}^3 \times c_p(v_{wind}) \quad (1)$$

where,  $P_w$ : Power generation of the wind (MW),  $\rho_{hub}$ : Air density at hub height ( $kg/m^3$ ),  $d_{rotor}$ : Rotor diameter of the wind turbine (m),  $v_{wind}$ : Wind speed (m/s),  $c_p(v_{wind})$ : Power coefficient of the wind turbine at the given wind speed.

#### D. Solar photovoltaic (PV)

To determine the potential electricity generation by PV, it is imperative to obtain the total global solar irradiation ( $G_i$ ) data for the specific geographic location of Dijon. To do so, Diffuse Horizontal Irradiance (DHI) and Direct Normal Irradiance (DNI) were obtained through the MERRA-2 data sources [23]. However, DNI and DHI were only utilized to derive the Global Horizontal Irradiance (GHI) data, as per the given equation.

$$GHI = DNI \times \cos(\theta) + DHI \quad (2)$$

where,  $\theta$ : Zenith angle

Once DNI, DHI, and GHI data were obtained, the open PVlib [25] library in Python was used to calculate the total global solar irradiation ( $G_i$ ) using the isotropic sky model. This model mathematically estimates the global solar radiation received by a PV module, assuming that the solar radiation is incident equally from all directions. Therefore, the total global solar irradiation on the module is the sum of direct and diffuse radiations received from all directions, considering an albedo of 0.20. PV module chosen to obtain the solar power had a unit-rated power of 0.11 MW, an azimuth angle of 180 degrees towards the south, and was tilted at an angle of 27.5 degrees with a maximum power temperature coefficient ( $\gamma$ ) of -0.5072 (%/°C). The cell temperature and PV power were then obtained using equations 3 and 4.

$$T_{cell} = T_{STC} + \frac{T_{NOCT} - 20}{800} \times G_i \quad (3)$$

$$P_{PV} = (1 + \gamma(T_{cell} - T_{STC})) \times \frac{G_i}{G_{STC}} \quad (4)$$

where,  $G_i$ : Total irradiance ( $W/m^2$ ),  $G_{STC}$ : Global irradiance at standard temperature condition ( $1000 W/m^2$ ),  $P_{pv}$ : Photovoltaic power (MW),  $T_{cell}$ : Module cell temperature (°C),  $T_{STC}$ : Cell temperature at standard condition (°C),  $T_{NOCT}$ : Nominal operating temperature condition (°C)

#### E. Battery (Bt) and Hydrogen ( $H_2$ ) system

The focus of this study revolved around  $H_2$  systems comprised of an electrolyzer, fuel cell, and  $H_2$  tank, serving as the conversion and storage elements, respectively. The electrolyzer utilizes electricity and water to generate hydrogen and oxygen. Specifically, an alkaline electrolyzer was chosen for this investigation due to its suitability for large-scale applications. However, it should be noted that the study did not consider the start-up, shutdown, or standby periods of the electrolyzer, assuming its continuous operation throughout the year. The  $H_2$  produced by the electrolyzer was initially intended to be compressed to 30 bar and subsequently compressed to 320 bar

TABLE I: Technical Parameters of the study

Components	Parameters		Sources
Solar Photovoltaic	Nominal Power	0.11 MW	[26]
Wind Onshore	Nominal Power	3.2 MW	[26]
Alkaline Electrolyzer	Nominal Power	2 MW	[26]
	Efficiency	66.5 %	[26]
Compressor (30-320 bar)	Nominal Power	0.2 MW	[26]
	Nominal Power	16.7 MWh	[26]
Hydrogen Tank (Compressed)	Charge efficiency	88%	[26]
	Discharge efficiency	100%	[26]
	Minimum state of charge	33%	Own assumption
	Maximum state of charge	100%	Own assumption
	Nominal Power	3.2 MWh	[26]
Battery	Charge efficiency	98%	[26]
	Discharge efficiency	97%	[26]
	Self-discharge	0.01	[27]
	Maximum state of charge	100%	Own assumption
	Minimum state of charge	33%	Own assumption
PEM Fuel Cell	Nominal Power	0.12 MW	[28]
	Efficiency	55%	[27]
Bi-directional Inverter	Efficiency	97%	[27]

TABLE II: Economic Parameters of the Study

Components	CAPEX (FIXED)	OPEX(FIXED)	Lifetime (years)	Sources
Solar Photovoltaic	0.1 €/M/MW	9000 €/MW/year	20	[26], [27]
Wind Onshore	1.12 €/M/MW	14000 €/MW/year	27	[26]
Alkaline Electrolyzer	0.75 €/M/MW	5% of CAPEX €/MW/year	25	[26]
Compressor(30-320 bar)	0.35 €/M/MW	4% of CAPEX €/MW/year	15	[28]
Hydrogen Tank (Compressed)	0.057 €/M/MWh	600 €/MW/year	30	[26]
Battery	1.042 €/M/MWh	540 €/MW/year	20	[26]
PEM Fuel Cell	2.25 €/M/MW	45000 €/MW/year	15	[28], [27]

using a compressor. The pressurized  $H_2$  was then stored in the  $H_2$  tank at 320 bar. The produced  $H_2$  got stored in the tank, with a minimum initial state of charge of 33%. Charging and discharging of the  $H_2$  storage were considered contingent upon the previous state of charge, and  $H_2$  demand was mainly met through  $H_2$  discharge from the tank. Additionally, the study incorporated the use of Li-ion batteries, known for their ability to address short-term electricity fluctuations, boasting a cycle life of 6000 hours and a charging and discharging efficiency of approximately 98%, 97%. The battery was considered to fulfill electricity demands that were not met by PV, wind, or grid sources. In this scenario, the self-discharge rate of the battery was estimated to be around 0.01%. Both storage components, the  $H_2$  tank, and the battery, were limited to a minimum state of charge of 33%. The study also explored the combination of  $H_2$  fuel cells as a means of compensating for electricity shortages arising from wind and photovoltaic sources. In the scenario when there is no need for a fuel cell,  $H_2$  is exclusively employed to meet the  $H_2$  demand discharging from the  $H_2$  tank, thereby minimizing investment,

operational, and maintenance costs typically associated with fuel cells. The evaluation of additional components such as AC/DC or DC/AC converters and expanders was carried out, taking into account an efficiency of 97% for AC/DC or DC/AC converters and close to 100% efficiency for the expanders. The technical and economic parameters for different components are shown in Tables I and II. The data mentioned in this paragraph are presented in Table I and are retrieved from two major sources [26], [28].

#### F. Economic model

The primary objective of this study is to minimize the total annual costs (TAC) associated with the analyzed HRES. Accordingly, the economic model of the system takes into account key economic parameters such as capital expenditure (CAPEX), annuity factor (AF), and operational/maintenance costs (OPEX). Additionally, other factors like commodity costs can be included. In this case, the study considers these costs to be part of the capital expenditure, encompassing expenses related to raw materials, manufacturing, transportation, and taxes for the components, except for the grid. In the

context of this study, no investment is considered for the grid due to the well-established grid infrastructure in Dijon, France. Therefore, the only cost incurred about the grid is the cost associated with its transmission and distribution, which is assumed to be 25.45 €/MWh. This value is derived from the average cost of grid electricity transmission and distribution in France, which amounts to around 28 USD/MWh, as reported by the International Energy Agency (IEA) in 2020 [29]. Given the exchange rate of 1€ = 1.10 USD, the equivalent cost is calculated as 25.45 €/MWh. However, it should be noted that if commodity costs are not accounted for in the model, their inclusion would be necessary to obtain a more accurate economic representation of the system. The mathematical formulation used for the simulation to determine the TAC is presented as follows:

$$TAC = (CAPEX \times AF) + OPEX \quad (5)$$

$$AF = \frac{i}{1 - (1 + i)^{-n}} \quad (6)$$

where CAPEX is the capital investment and OPEX is the operation and maintenance costs. OPEX is sometimes expressed as a fraction of the overall capital costs. AF is the annuity factor which in this case calculates the equivalent annual cost of the capital investment over its useful lifetime. Along with this, interest rates also impact the economy of HRES. Having a low interest rate enhances the economic viability of the system which increases the chance of internal rate of return (IRR) and reduces the payback period which is majorly noticed by investors, stimulating the development and deployment of HRES technologies. In this study, the economic interest rate (i) is set at 8% over the economic lifetime (n).

### III. SIMULATION/OPTIMIZATION FORMULATION:

To achieve the objective, simulation, and optimization of the energy system were performed using FINE (Flow-based Integrated Network Environment), an open-source Python module [16]. FINE is a powerful and flexible optimization tool specifically designed for power system modeling and analysis, built on the Pyomo optimization framework. It provides a wide range of functions for modeling, simulation, and optimization of complex power systems, including electricity, gas, and heat networks. The optimization process within the FINE module aims to minimize the total annual costs (TAC) of the power system. The optimization model accounts for various constraints such as energy balance, power generation, conversion, storage, and transmission technology over a specified time horizon and spatial domain. Mathematical modeling and the formulation of the optimization problem are discussed in detail by Welder et al.[16].

In this study, the optimization process involved using time series data such as power profiles (PV, wind), load profiles (electric, H<sub>2</sub>), and techno-economic parameters to construct an energy system model in the FINE module. All technologies

were located in one node, and the temporal resolution was 1 hour over 1 year with 8760 hours of the time-step. To reduce the size of the data sets, we employed time series aggregation (TSA) specifications with typical periods and a clustering method. Typical periods were used to summarize and condense large time series data into smaller sets that represent typical patterns and behaviors, thereby simplifying data analysis. The FINE module offers various clustering methods such as k-means, exact k-medoids, hierarchical, and average. We used hierarchical clustering with a typical period of 100 typical days to enhance computing performance. However, we acknowledged that the accuracy of the optimization results may decrease when using a typical period of less than 100 days. In the simulation, the optimizer adjusts the capacity of each component to meet the system's requirements and operate at its optimal capacity, ensuring that energy demands are met. The simulation is based on mixed integer linear programming (MILP) integrated inside the FINE module and is being solved using Gurobi<sup>TM</sup> version 10.0.1 solver in the open programming interface of Spyder, python 3.9. The simulation is being run on a personal laptop of Mark DELL, 11th Gen Intel<sup>TM</sup> Core<sup>TM</sup> i5-1145G7 @ 2.60GHz. The optimal solution is obtained for the first, second, and third cases in 4.99, 14, and 189 seconds respectively.

### IV. RESULTS AND DISCUSSIONS:

#### A. Operation of the components in 3 different cases

The operation of components in the various case studies varied as determined through simulation and optimization. In Case I, the grid is considered the sole source of power. It is evident that the entire electric power demand of Dijon was satisfied by the grid, as depicted in Fig 4(a). Furthermore, the grid was responsible for meeting the electricity requirements to power the electrolyzer and compressor, utilized for H<sub>2</sub> production, compression of H<sub>2</sub> to 320 bar, and storage in the H<sub>2</sub> tank. The H<sub>2</sub> tank in response, discharged H<sub>2</sub> to meet the daily H<sub>2</sub> demand for transportation, particularly during the peak hours from 5 a.m to 10 a.m. H<sub>2</sub> tank undergoes charging during the night, reaching its high State of Charge (SOC) before the commencement of refueling activities, as illustrated in Fig 4(b). In Case II, the study examined the integration of PV, and WT, in conjunction with the power grid. In Fig 5(a), the operational dynamics of PV, WT, and the grid are depicted with electricity and H<sub>2</sub> loads for 20 days of January to observe the operation of the system components and grid during the high electricity demand and less production of renewable energy. Notably, it is discernible that during periods of insufficient wind and solar power generation, the grid effectively compensated for the deficit, ensuring a continuous and reliable power supply. The state of the H<sub>2</sub> tank and the discharge of the H<sub>2</sub> tank remained approximately the same between Case I and Case II regardless of the power sources utilized in each case. Battery and Fuel cells are not visibly operated because of the

presence of the grid to ensure the electricity and electrolyzer power demands to fulfill the electricity and production of  $H_2$ . The  $H_2$  tank undergoes charging during the overnight period to facilitate the subsequent discharge of hydrogen in the refueling process that takes place in the morning as depicted in Fig 5(b).

In Case III, the focus of the study was on evaluating an off-grid system. The operation of PV and WT, as illustrated in Fig 6(a), aimed to meet all essential demands. However, due to the inherent intermittency in renewable sources, it became necessary to incorporate discharge from the battery (Bt) and activate the fuel cell to ensure a consistent power supply. Consequently, Fig 6(a) vividly captures both the charge and discharge cycles of the Bt, as well as the corresponding charge and discharge cycles of  $H_2$  tank, offering insights into the system's operation over approximately 20 days of January. The surplus renewable power generated is efficiently employed in dual processes: charging the Bt and producing  $H_2$  while simultaneously filling the  $H_2$  tank. This strategic utilization ensures that the Bt is available for short-term energy needs, mitigating abrupt fluctuations, while the stored  $H_2$  serves as a reservoir for addressing more prolonged seasonal power variations. The observational data indicates that, in tandem with these charging and discharging activities within the storage devices, the overall energy demands are consistently met. Fig 6(b) reveals that the SOC of the  $H_2$  tank was highest in July and August (180-250 days), coinciding with peak PV and wind power production. However, daily charging and discharging of the  $H_2$  tank were necessary due to the refueling requirements of vehicles. This highlights the continuous utilization of the  $H_2$  tank to meet transportation needs, even during months with abundant renewable energy production.

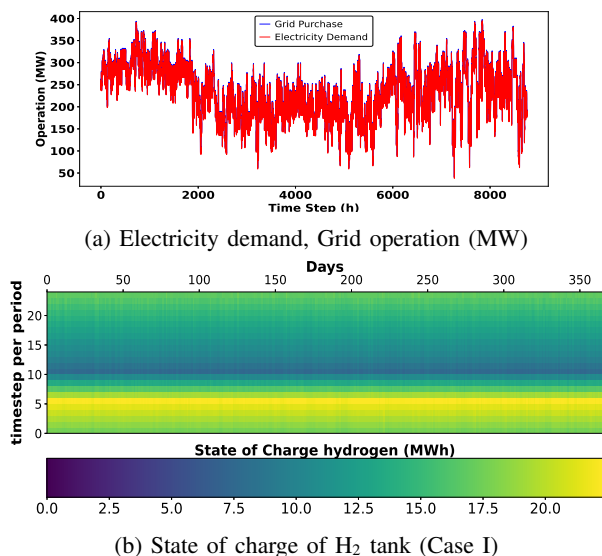
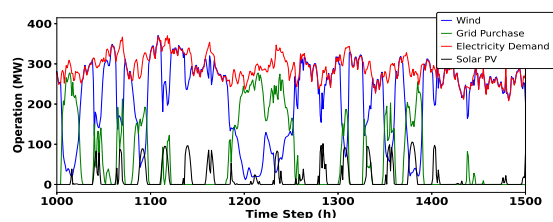
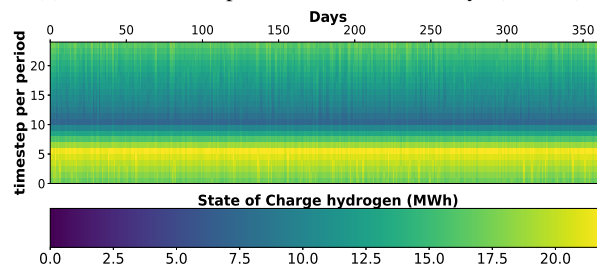


Fig. 4: Operation of grid,  $H_2$  state of charge in Case I



(a) PV, WT, Grid operations of about 20 days (Case II)



(b) State of charge of  $H_2$  tank (Case II)

Fig. 5: Hydrogen tank state of charge in Case II

### B. Economic analysis in three various cases

In Case I, where the grid exclusively served as the primary energy source, the total annual cost (TAC) was contingent solely on the distribution and transportation of grid power, resulting in a substantial TAC of 52.82 million € (€M), as illustrated in Fig 7(b).

It is worth noting, however, that the cost of grid electricity is susceptible to volatile spot prices, which could significantly impact the TAC. While this analysis did not take into account the fluctuations. From Fig 7(a), it is evident that in Case I, the investment in the electrolyzer,  $H_2$  tank, and compressors comprise a significant proportion, given that no specific investment in the grid was considered. Nevertheless, when accounting for investments in the grid and fluctuations in electricity prices, the TAC may experience variations. Notably, this study suggests that employing grid electricity for  $H_2$  production could be a viable option in Dijon, as France reportedly exempts tariffs for electrolyzer-based  $H_2$  production via the grid. However, to foster energy sustainability and reduce dependency on the grid, it is advisable to enhance the integration of renewable sources like wind and PV, alongside  $H_2$  and Bt storage.

In Case II, the incorporation of renewable energy sources (PV, WT) had a favorable impact on the TAC and the management of supply and demand, alleviating strain on the grid. The results of Case II demonstrated that with the grid operation alongside WT and PV, the TAC for the PV and WT amounted to 119.51 and 34.93 €M. This was accompanied by an additional investment of 500 and 336 €M as depicted in Fig 7(a). Moreover, the TAC for the grid stood at 8.21 €M, reflecting an impressive reduction of approximately 84% compared to Case I, where the grid functioned as the sole

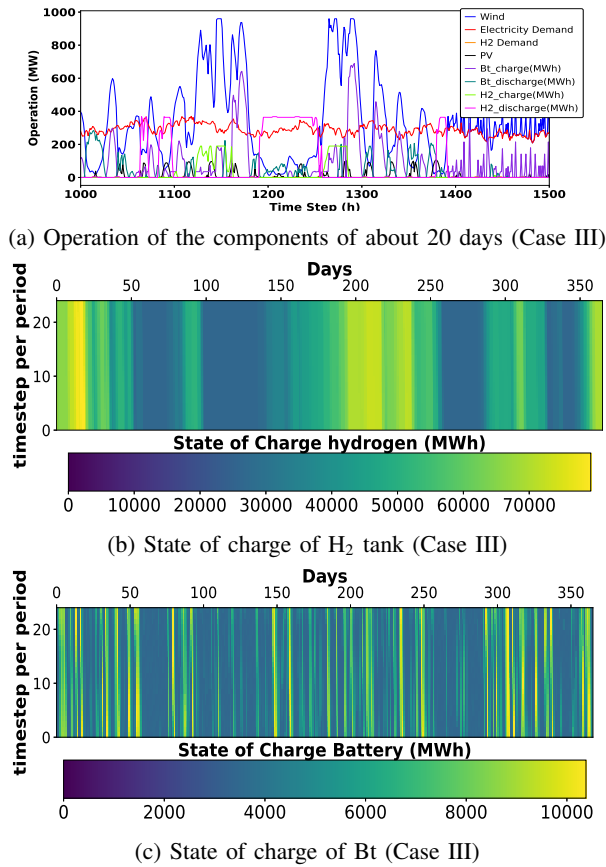
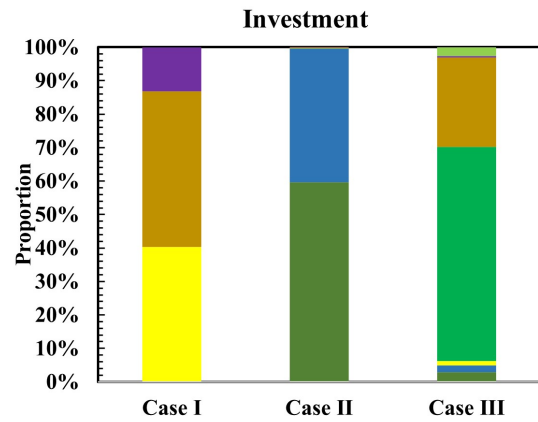


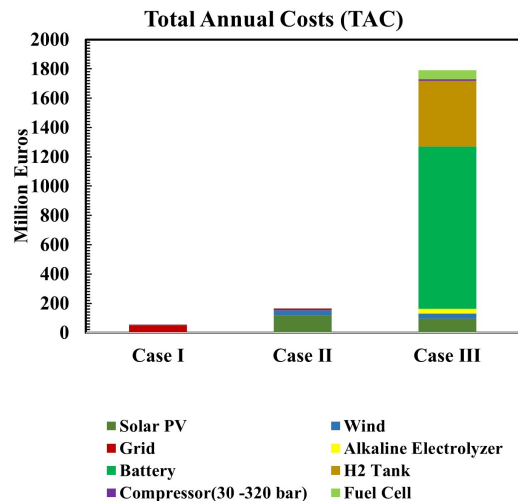
Fig. 6: Operation of the components in Case III

power source. In Case I, the overall investment for the system was estimated at a mere 2.7 €M, with roughly 40% and 45% of the investment allocated to the electrolyzer and H<sub>2</sub> tank, as showcased in Fig 7(a). In contrast, the presence of renewable in Case II significantly raised the total system investment to 838 €M, with over 90% of the investment dedicated to the PV and WT, as illustrated in Fig 7(b).

Case III, focusing on an off-grid scenario, exhibited a noteworthy escalation in the TAC for the entire system, as demonstrated in Fig 7(b). This increase can be attributed to substantial investments, operation, and maintenance costs associated with various components, necessary to meet the electricity and H<sub>2</sub> demand. The utilization of fuel cells and Bt to support the WT and PV during peak demand to regulate supply and demand further elevated the TAC for the Bt, H<sub>2</sub> tank, and fuel cell in this particular scenario. This stands in contrast to Case II and Case I, where the grid was present, and the Bt and fuel cell were not in operation. Consequently, the TAC and investment for the H<sub>2</sub> tank and Bt surpassed those of the other components. The additional investment accounted for the larger capacity required to store the excess electricity and H<sub>2</sub> generated during surplus periods, which can then be used to meet the demand during deficits.



(a) Investment



(b) Total Annual Costs (Million €)

Fig. 7: Investment and TAC in various cases

## V. CONCLUSION AND FUTURE WORK

In conclusion, the study emphasizes the substantial cost advantages of relying solely on the grid. However, to alleviate grid stress, reduce carbon emissions associated with grid energy import, and prioritize renewable sources (PV, WT), the integration of PV, WT, and the grid was explored. This approach demonstrated a noteworthy reduction in the Total Annual Cost (TAC) of the system, effectively managing the complex dynamics of supply and demand. Using grid power involves carbon emissions, but in the case of France, those are lower than in other countries due to the nuclear power part in the electricity mix. Further studies could explore the impact of carbon penalties on the cost of importing grid energy, the life cycle analysis of the system components, explore the ways to decrease dependence on the grid or reduce carbon emissions

through multi-objective scenarios, providing more sustainable energy approaches. Furthermore, the study underscores the promising prospects of H<sub>2</sub> components and Bt as economically viable storage solutions in forthcoming energy scenarios. Bt demonstrates cost-effectiveness in managing short-term power fluctuations. Although fuel cells currently entail higher costs for power provision, advancements in fuel cell technology hold the potential for more affordable power solutions in the forthcoming years. Moreover, the study showcases the potential of the electrolyzer and H<sub>2</sub> tanks for cost-effective H<sub>2</sub> production and storage, serving refueling stations to fulfill daily transportation fuel requirements. The continuous progress in electrolyzer and H<sub>2</sub> tank technologies is expected to drive down costs shortly. The study also emphasizes the value of utilizing the FINE module integrated with the Python interface as a valuable tool for analyzing hybrid renewable energy systems. However, it is crucial to note that the current version of FINE lacks features addressing multiple objectives. In future studies, multiple objectives such as reducing carbon emissions, mitigating grid dependency, reducing power loss produced by renewable generation, selling of the H<sub>2</sub> or electricity, increasing renewable penetration, etc. can be considered.

#### ACKNOWLEDGMENT

This work has been supported by the EIPHI Graduate School (contract ANR-17-EURE-0002), by the Region Bourgogne Franche-Comté, and by the ISITE BFC (contract ANR-15-IDEX-003).

#### REFERENCES

- [1] A. Henriot, "Economic curtailment of intermittent renewable energy sources," *Energy Economics*, vol. 49, pp. 370–379, 5 2015.
- [2] S. Basnet, K. Deschinkel, L. Le Moyne, and M. C. Péra, "A review on recent standalone and grid integrated hybrid renewable energy systems: System optimization and energy management strategies," *Renewable Energy Focus*, 2023.
- [3] J. Liu, S. Cao, X. Chen, H. Yang, and J. Peng, "Energy planning of renewable applications in high-rise residential buildings integrating battery and hydrogen vehicle storage," *Applied Energy*, vol. 281, p. 116038, 2021.
- [4] R. Babaei, D. S. Ting, and R. Carriveau, "Optimization of hydrogen-producing sustainable island microgrids," *International Journal of Hydrogen Energy*, vol. 47, no. 32, pp. 14375–14392, 2022.
- [5] L. Li, J. Wang, X. Zhong, J. Lin, N. Wu, Z. Zhang, C. Meng, X. Wang, N. Shah, N. Brandon, *et al.*, "Combined multi-objective optimization and agent-based modeling for a 100% renewable island energy system considering power-to-gas technology and extreme weather conditions," *Applied Energy*, vol. 308, p. 118376, 2022.
- [6] J. D. Fonseca, J.-M. Commenge, M. Camargo, L. Falk, and I. D. Gil, "Multi-criteria optimization for the design and operation of distributed energy systems considering sustainability dimensions," *Energy*, vol. 214, p. 118989, 2021.
- [7] Q. H. Goh, L. Zhang, Y. K. Ho, and I. M. L. Chew, "Modelling and multi-objective optimisation of sustainable solar-biomass-based hydrogen and electricity co-supply hub using metaheuristic-topsis approach," *Energy Conversion and Management*, vol. 293, p. 117484, 2023.
- [8] D. Cho and J. Valenzuela, "A scenario-based optimization model for determining the capacity of a residential off-grid pv-battery system," *Solar Energy*, vol. 233, pp. 478–488, 2022.
- [9] A. Maleki and F. Pourfayaz, "Sizing of stand-alone photovoltaic/wind/diesel system with battery and fuel cell storage devices by harmony search algorithm," *Journal of Energy Storage*, vol. 2, pp. 30–42, 2015.
- [10] C. Mokhtara, B. Negrou, N. Settou, A. Boufferrouk, and Y. Yao, "Design optimization of grid-connected pv-hydrogen for energy prosumers considering sector-coupling paradigm: Case study of a university building in algeria," *International Journal of Hydrogen Energy*, vol. 46, no. 75, pp. 37564–37582, 2021.
- [11] A. C. Duman and Önder Güler, "Techno-economic analysis of off-grid pv/wind/fuel cell hybrid system combinations with a comparison of regularly and seasonally occupied households," *Sustainable Cities and Society*, vol. 42, pp. 107–126, 2018.
- [12] M. M. Samy, M. I. Mosaad, and S. Barakat, "Optimal economic study of hybrid pv-wind-fuel cell system integrated to unreliable electric utility using hybrid search optimization technique," *International Journal of Hydrogen Energy*, vol. 46, no. 20, pp. 11217–11231, 2021.
- [13] R. M. Elavarasan, S. Leoponraj, A. Dheeraj, M. Irfan, G. G. Sundar, and G. Mahesh, "Pv-diesel-hydrogen fuel cell based grid connected configurations for an institutional building using bwm framework and cost optimization algorithm," *Sustainable Energy Technologies and Assessments*, vol. 43, p. 100934, 2021.
- [14] H. Mehrjerdi, "Off-grid solar powered charging station for electric and hydrogen vehicles including fuel cell and hydrogen storage," *International journal of hydrogen Energy*, vol. 44, no. 23, pp. 11574–11583, 2019.
- [15] S. Turkdogan, "Design and optimization of a solely renewable based hybrid energy system for residential electrical load and fuel cell electric vehicle," *Engineering Science and Technology, an International Journal*, vol. 24, no. 2, pp. 397–404, 2021.
- [16] L. Welder, D. S. Ryberg, L. Kotzur, T. Grube, M. Robinius, and D. Stolten, "Spatio-temporal optimization of a future energy system for power-to-hydrogen applications in germany," *Energy*, vol. 158, pp. 1130–1149, 9 2018.
- [17] International Renewable Energy Agency, "Renewable power generation costs in 2020," 2021.
- [18] Hydrogen Council, "Path to hydrogen competitiveness: A cost perspective," 2021. Accessed: May 5, 2023.
- [19] "Open Data Réseaux Énergies (ODRÉ)," 2023. Accessed: May 5, 2023.
- [20] McPhy, "Dijon Metropole Smart Energy (DMSE)." <https://mcphy.com/fr/realisations/mobilite-hydrogene/dijon-metropole-smart-energie-dmse/>, Accessed on 2023-05-08.
- [21] V. Oldenbroek, S. Wijtzes, K. Blok, and A. J. van Wijk, "Fuel cell electric vehicles and hydrogen balancing 100 percent renewable and integrated national transportation and energy systems," *Energy Conversion and Management*: X, vol. 9, 3 2021.
- [22] GE General Electric, "GE General Electric - Wind Turbine Manufacturer," 2023. Accessed: May 5, 2023.
- [23] M. M. Rienecker, M. J. Suarez, R. Gelaro, R. Todling, J. Bacmeister, E. Liu, M. G. Bosilovich, S. D. Schubert, L. Takacs, G. K. Kim, *et al.*, "Merra: Nasa's modern-era retrospective analysis for research and applications," *J Clim*, vol. 24, no. 14, pp. 3624–3648, 2011.
- [24] wind-python, "The windpowerlib is a library to model the output of wind turbines and farms." GitHub repository, 2023. Accessed: May 5, 2023.
- [25] "Github - pvlib/pvlib-python: A set of documented functions for simulating the performance of photovoltaic energy systems.."
- [26] Energistyrelsen, "Technology Data." Website, 2023. Accessed: May 5, 2023.
- [27] K. Knosala, L. Kotzur, F. T. Röben, P. Stenzel, L. Blum, M. Robinius, and D. Stolten, "Hybrid hydrogen home storage for decentralized energy autonomy," *international journal of hydrogen energy*, vol. 46, no. 42, pp. 21748–21763, 2021.
- [28] J. Arnal and L. Glielmo, "Environmental performance analysis revision history," 2023.
- [29] International Energy Agency, "Electricity transmission and distribution in a decarbonised world," technical report, International Energy Agency, 2020.